Journal of Engineering Science and Technology
EURECA 2014 Special Issue April (2015) 1 - 14

DESIGN EVALUATIONS OF THE NOVEL DOUBLE ROTOR SWITCHED RELUCTANCE MACHINE

ARAVIND CV[1,*], REYNOLD HARIYADI[1], A.JAGADEESWARAN[2]

[1]School of Engineering, Taylor's University, Taylor's Lakeside Campus,
No. 1 Jalan Taylor's, 47500, Subang Jaya, Selangor DE, Malaysia
[2]Sona SPEED, Salem, India
*Corresponding Author: aravindcv@ieee.org

Abstract

The need of magnet-less machine for industrial applications are increasing, and one of the most common magnet-less machine is switched reluctance machine. Switched reluctance machine utilises the basic concept of attraction and repulsion principle, and together with the air-gap reduction an improvement in the production of the torque generation is separated earlier. The concept of dual air-gap to improve the torque density of the switched reluctance machine is attempted by researchers in recent times. The concept of dual air-gap shows a high starting torque density in the machine which allows an early steady state in the machine performance compared to the conventional machine. As the drawback, the dual air-gap machine is not able to produce higher torque average and drags is presence for industrial application. Therefore, a novel through modification of magnetic circuit of the dual air-gap in double rotor switched reluctance machine is proposed. In this paper, a comparison in terms of motor torque constant square density between three machines of conventional switched reluctance machine (SRM), double rotor switched reluctance machine (DRSRM), and the proposed dual air-gap machine is presented. The results shows that there is an improvement in the average torque by 13% compare to the SRM and 39% compare to the DRSRM. The proposed dual air-gap machine, it is also showing an improvement in motor constant square density by 37% and 114% of SRM and DRSRM, respectively.

Keywords: Dual air-gap, Double rotor, Switched reluctance, Motor constant, Square density, Torque generation.

1. Introduction

The first machine around 1830s with the based concept of electromagnet was reluctance machine. The reluctance machine has certain novel features and its

Nomenclatures

ℓ_{g1}, ℓ_{g1}	Length of air-gap, m
R_{g1}, R_{g2}	Radius of air-gap, m
h_c	Height of the coil, m
l_r	Length of the rotor flux, m
l_{rc}	Length of the rotor core, m
l_g	Length of the air gap, m
n_c	Number of coil turn
n_{cnett}	Nett coil turns
w_c	Width of the coil, m
A_s	Area of stator pole, m^2
A_{sp}	Area of stator pole base, m^2
A_y	Area of yoke surface, m^2
A_{rt}	Area of rotor tooth, m^2
A_R	Net area of rotor , m^2
A_{rc}	Area of rotor core, m^2
A_g	Area of the air gap, m^2
A_s	Area of stator pole, m^2
A_{st}	Area of stator pole tooth, m^2
B_{av}	Specific magnetic loading, wb/m^2
B_r	Rotor magnetic flux density, wb/m^2
B_s	Stator magnetic flux density, wb/m^2
C_{sy}	Stator back iron thickness, m
C_{ry}	Rotor back iron thickness, m
C_y	Net yoke back iron, Tesla
C_0	Output coefficient
D_{sh}	Shaft diameter, m
D	External diameter, m
D_o	Exterior diameter, m
H_g	Magnetic flux intensity, At/m
I_z	Current in the coil, A
L	Stack length, m
N_s	Synchronous speed, rpm
P_d	Developed power, syn-watts
Q	Generator capability
R_g	Reluctance in the air gap, At/wb
W_s	Width of the stator, m
Z	Total number of coils

Greek Symbols

$\Re_{g1}$	Reluctance in the air-gap1
$\Re_{g2}$	Reluctance in the air-gap 2
$\emptyset_r$	Flux in the rotor, wb
μ_0	Permeability of free space, H/m
μ_r	Relative Permeability, H/m
η_m	Machine efficiency

reinvention has brought new possibility due to the inexpensive and high power switching devices [1]. It has a simple structure in comparison to the induction or synchronous machine. There are many applications which has been developed

through the basic understanding of switched reluctance machine such as, for elevator application [2], washing machine [3], and wind application [4].

In this present day, the need for switched reluctance machine is increasing, because of the skyrocketing price for rare earth magnets. Most researchers nowadays are trying to improve torque output capability in a wide range of speed operating system in which has the high fault tolerance capabilities [5-6]. The optimizations of the reluctance machine design for industrial applications are important. There are many different approached for the improvement of reluctance machine attempted by various researchers such as, it can be done by torque ripple minimization [7-8], current control [9], or structural and mechanical parameter optimization [10].

In order to produce an improvised switched reluctance machine design, using dual air-gap the guideline and presented in [11-13] is utilized. The switched reluctance machine which previously developed in [11-12] is evaluated. Also the previous SRM and DRSRM are designed and analyzed through numerical tool. It has been identified that the torque generation in conventional switched reluctance machine is depends on the air-gap distance between rotor and stator; and from the basic concept of reduction in the air-gap area, a double rotor switched reluctance machine [13] which has the dual air-gap magnetic circuit with modified magnetic circuit is introduced. The previous dual air-gap magnetic circuit shows that the torque generation characteristics in the machine performance has a high starting torque and it reaches its steady state much faster compare to the conventional switched reluctance machine. However, there is drawback in the previous double rotor switched reluctance machine designed, where the machine volume is much higher compare to the conventional machine and the torque produces is lower. Although there are some drawbacks, the dual air-gap magnetic circuit has open the possibility for switched reluctance machine to advance in the used of industrial applications. In this paper, a dual air-gap through a new magnetic circuit is proposed [14-15], a novel design of double rotor switched reluctance machine with a higher torque generating capability is introduced. In order to identify the performance of the proposed machine, finite element analysis is presented and motor constant square density is used as evaluation parameters of all the machines with same volume and size are being compared. From this analysis, it is shows significant changes the percentage improvement of the proposed machine compared to the previous machine designs.

2. Design Methodology

2.1. Design Concepts

2.1.1. Sizing of the machine

As the operation of reluctance machine lies in the basic principle of attraction and repulsion. The torque generation capabilities of the reluctance machine is produce in the air-gap of the electromagnetic force. The generation of magnetic flux in Double Rotor Switched Reluctance Machine is given in the Eq. (1) as,

$$NI = \phi(\Re_{g1} + \Re_{g2}) \tag{1}$$

where ϕ is the magnetic flux, N is number of turns, I is current, $\Re_{g1}$ and, $\Re_{g2}$ are

air-gap magnetic reluctance. The $\Re_{g1}$ of the dual air-gap magnetic design $\Re_{g1}$ is given in Eq. (2),

$$\Re_{g1} = \frac{\ell_{g1}}{\pi \mu_o {r_{g1}}^2} \tag{2}$$

where ℓ_{g1} is the length of the first air-gap, μ_o is the material permeability, and r_{g1} is the first air-gap radius. The $\Re_{g2}$ of the dual air-gap magnetic design $\Re_{g2}$ is given in Eq. (3),

$$\Re_{g2} = \frac{\ell_{g2}}{\pi \mu_o {r_{g2}}^2} \tag{3}$$

where ℓ_{g2} is the length of the second air-gap, and r_{g2} is the second air-gap radius. The magnetic circuit used in the dual air-gap of the double rotor switched reluctance machine is designed from the Eq. (1) – Eq.(3) are presented in Fig.1.

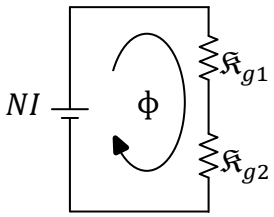

Fig. 1.Equivalent Machine Magnetic Circuit.

The structural dimension of the proposed dual air-gap switched reluctance machine for dual air-gap machine design of the proposed double rotor switched reluctance machine is presented in Fig 2

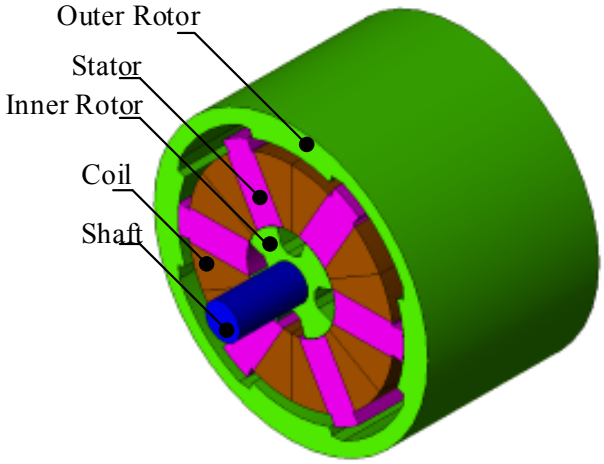

Fig. 2.Proposed Double Rotor Switched Reluctance Machine.

2.1.2. Stator design

The design of the stator polefor this machine is shown in Fig. 2.The area of the pole (A_s) is found using Eq.(4).

$$A_s = \frac{D}{2} L A_{st} \tag{4}$$

The area of the middle pole(A_{sp}) is found using Eq.(5)- Eq.(7).

$$A_{sp} = W_s L \tag{5}$$

$$A_{st} = A_s + A_{sp} \tag{6}$$

$$\emptyset_s = A_{st} B_s \tag{7}$$

Therefore the net flux ($\emptyset_y$) present in the yoke is found using Eq.(8).

$$\emptyset_y = \frac{\emptyset_s}{2} = \frac{A_{st} B_s}{2} \tag{8}$$

Assume that the flux density of the yoke ($\emptyset_y$)equals to half the flux density of the stator ($\emptyset_s$), the flux density is shown in Eq.(9) -Eq.(11).

$$\emptyset_y = A_y B_y \tag{9}$$

$$\emptyset_y = \frac{A_y B_s}{2} \tag{10}$$

$$A_{st} = A_y \tag{11}$$

The thickness of the stator back iron (C_{sy}) is found using Eq.(12)- Eq.(13).

$$C_{sy} = \frac{A_y}{L} \tag{12}$$

The width of the stator is found using Eq.(13):

$$W_s = L \times 0.7 \tag{13}$$

2.1.3. Rotor design

The outer rotor and inner rotor back iron thickness are implanted on the basic principle and operating flux density. The ideal back iron thickness range of value in outer rotor can be obtain if some conditions are taken into consideration during the machine design such as, the air-gap inter-polar is getting larger, the inductance between aligned and unaligned position gives a high ratio value; and the shorter the rotor poles, it could help to reduce the vibration in the machine performance. Based on the design consideration above, the range design value in back iron thickness of the outer rotor b_{ory} is presented in Eq.(14).

$$0.25\omega_{sp} < b_{ory} < 0.5\omega_{sp} \tag{14}$$

The outer rotor pole height h_{or} is presented in Eq.(15).

$$h_{or} = \left[\frac{D_{is} - 2(\ell_{og} + \ell_{ig}) - D_{sh} - 2b_{ory} - 2b_{iry}}{2}\right] \tag{15}$$

where ℓ_{og} is the outer air-gap length between outer stator and outer rotor, ℓ_{ig} is the inner air-gap length between inner rotor and inner stator. The outer rotor middle pole height $h_{orm}$is in Eq.(16)

$$h_{orm} = 2\pi\left(r_{orms}\frac{\theta_{uor}}{360} - (r_{oris} + h_{or})\frac{\theta_{mor}}{360}\right) - \frac{\theta_{orm}}{360} \tag{16}$$

where θ_{orm} is the outer rotor middle angle. The ideal back iron thickness range of value in inner rotor is having similar design consideration with the outer rotor. In the inner rotor design, the range design value for back iron thickness of the inner rotor b_{iry} is given in Eq.(17).

$$0.2\omega_{sp} < b_{iry} < 0.4\omega_{sp} \tag{17}$$

The inner rotor pole height h_{ir} is presented in Eq.(18).

$$h_{ir} = \left[\frac{D_{is} - 2\ell_{ig} - D_{sh} - 2b_{iry}}{2}\right] \tag{18}$$

The inner rotor middle lower height h_{irml} is presented in Eq.(19).

$$h_{irml} = 2\pi(r_{irms} + h_{ir})\frac{\theta_{irml}}{360} \tag{19}$$

where θ_{irml} is the inner rotor middle lower angle. The inner rotor middle upper height is presented in Eq.(20).

$$h_{irmu} = 2\pi(r_{irms} + h_{ir} + h_{irml})\frac{\theta_{irmu}}{360} \tag{20}$$

where θ_{irmu} is the inner rotor middle upper angle.

2.1.4. Yoke design

The mean path lengths for different parts are found using Eq.(21) – Eq.(22).

$$l_r = h_r + \frac{C_y}{2} \tag{21}$$

$$l_{rc} = (\pi)\left(\frac{D_o}{2} - \frac{C_y}{2}\right) \tag{22}$$

The flux density present in the air gap is found using Eq.(23).

$$B_g = \frac{A_s B_s}{A_g} \tag{23}$$

The magnetic field intensity present in the air gap is found using Eq.(24).

$$H_g = \frac{B_g}{4\pi \times 10^{-7}} \tag{24}$$

2.1.5. Shaft Design

In a machine, the shaft is responsible for transmitting power from one rotating part of the machine to another rotating part of the machine. The shaft also acts as a support structure for the rotating parts of a machine like the rotor and the permanent magnets in this case. The diameter of the shaft is designed using Eq. (25).

$$D_{sh} = (0.55)\left(\frac{P_d}{\omega}\right)^{\frac{1}{3}} \tag{25}$$

2.1.6. Winding design

The dimensions of the coil are chosen based on the Imperial Standard Wire Gauge (SWG) where 21 SWG has 0.813mm diameter. The area of winding ($A_{1,2}$) around the stator slot is presented in Eq.(26).

$$A_{1,2} = \pi (r_{1,2})^2 \frac{\theta_{1,2}}{360^\circ} \tag{26}$$

where the parts of the area winding is A, r is the radius, θ is the angle of the winding. The total area winding per pole (A_{ca})is presented in Eq.(27).

$$A_{ca} = A_1 - A_2 \tag{27}$$

The area cross section of the coil (A_{coil})is presented in Eq.(28).

$$A_{coil} = \pi {r_{coil}}^2 \tag{28}$$

The number of turns of the coil in each stator pole (T_{ph})can be identified from the Eq.(29).

$$T_{ph} = \left(\frac{A_{ca}}{A_{coil}}\right) \times 60\% \tag{29}$$

Figure 3 show the coil design used in this research and Fig. 4 shows the complete structure of the designed machine.

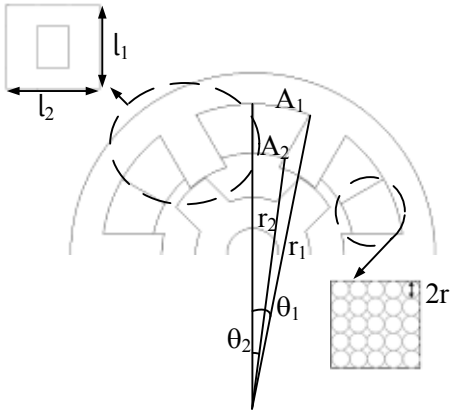

Fig. 3. Coil Design.

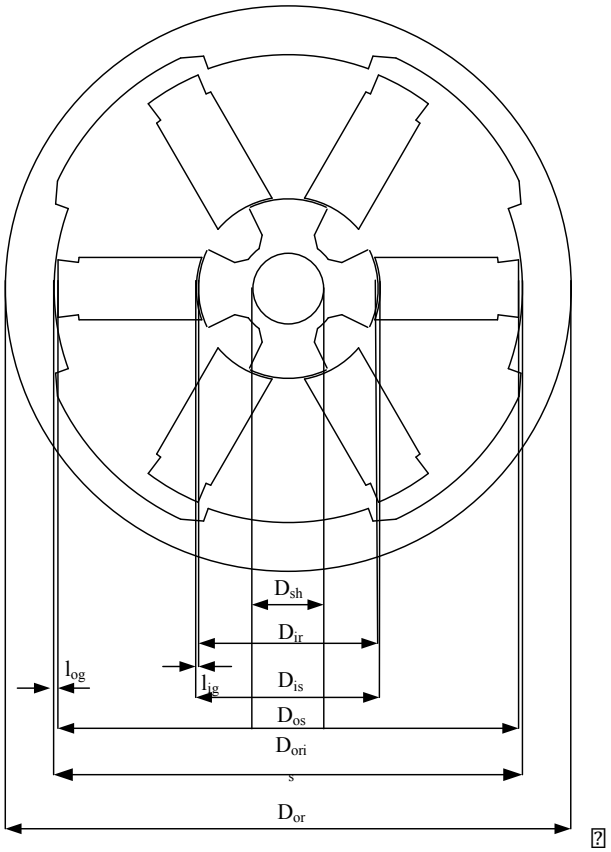

Fig 4. Complete Design.

3. Numerical Analysis

3.1. Finite Element Analysis (FEA)

In this research the finite element analysis of the machine design analysis uses industrial standard FEA tools [11-13]. The proposed machine magnetic flux characteristics are presented in Fig.5.The magnetic flux at different positions between the stator core and double rotor core are presented. In this condition, when the machine at aligned position, the magnetic flux produces at its maximum. As the rotor starts to move further away from the initial position at 0°, the magnetic flux is gradually decrease and at the same time the torque is starts to generate, and then when the rotors reaches its complete unaligned position the flux linkage is reached its minimum constant value.

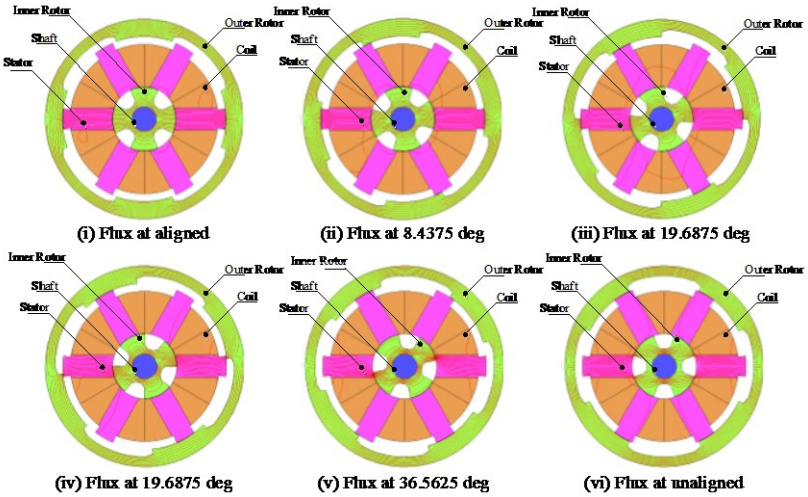

Fig. 5.Analysis for various Rotor position.

3.2. Figures of Merit

For comparison on the level of performance for conventional and proposed structure, the methods of calculation Motor Constant Square Density G is used. This evaluation is very useful as it includes the torque, power, and volume of the machine designs. The Motor Constant Square Density G is given as in Eq.(30).

$$G = \frac{(K_m)^2}{V} \tag{30}$$

where K_m is the machine constant in $[Nm/A/W^{-(1/2)}]$, V is the volume of the machine $[m^3]$. The machine constant can be further expressed as in Eq. (31).

$$K_m = \frac{K_T}{\sqrt{P}} \tag{31}$$

where K_T is the torque constant $[Nm/A]$ and P is the input power to the coil winding $[W]$. The torque constant is given as in Eq.(32).

$$K_T = \frac{T_{avg}}{I} \tag{32}$$

where T_{avg} is the fundamental torque $[Nm]$ and I is the maximum current input to the machine $[A]$.

4. Results and Discussions

4.1. Dynamic characteristics

Dynamic characteristics are important for studying the state of the machine under the normal operating condition with load. In the dynamic characteristics experiment the excitation state is created based on the alternating conditions between opening and closing switches in accordance with the position of the rotor's rotation. The torque waveform of dynamic characteristicas shown in Fig.6, when the voltage application width θ_w is 30 deg with the changing voltage application θ_s starts $-5\ deg$, 0 deg, and 5 deg. The results shows that the changing application at $-5\ deg$ in application width of30 deg, gives high torque generations compare to other changing voltage applications. From these experimental results it can be explained that the best voltage time changes for the circuit controller is 5 degree early within the 30 degree application ranges.

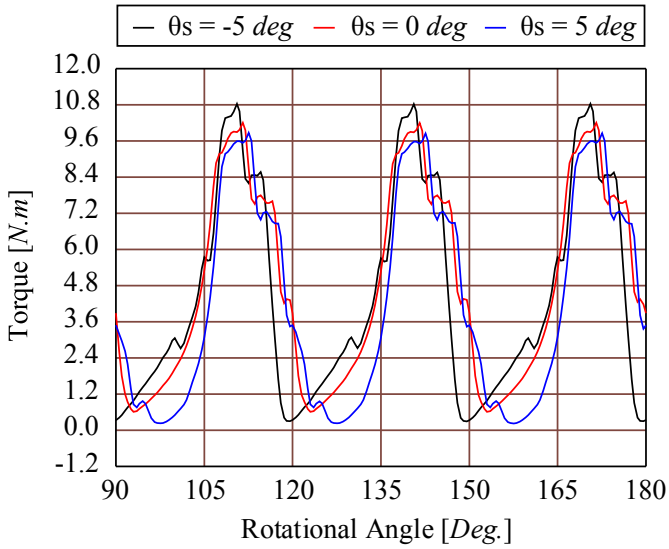

Fig.6.Torque Characteristics (θ_w: 30 deg)

4.2. Drive characteristics

These types of machines require electronic control drive in order to operate at the operational condition. In the drive characteristics experiment the physical phenomena analysis of the magnetic circuit and drive circuit is created, where both is used to create a torque analysis model.

The circuit diagram which designed for this analysis contains a voltage source and an ON/OFF square wave voltage of three-phase switching is controlled depending on the timing settings. Fig. 7 shows that whether the iron loss is taken

into account or not, it shows no effect on the torque production because of the iron loss ratio to output is small.

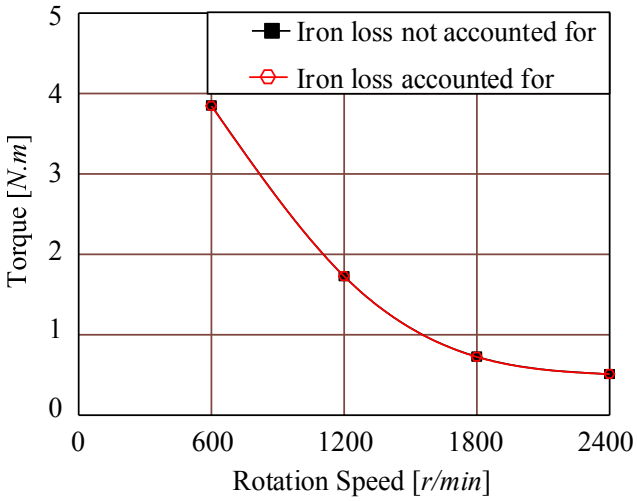

Fig. 7.Speed torque characteristics.

In the current characteristics experiment the physical phenomena analysis of the magnetic circuit is created using torque analysis model for the simulation of the circuit model from the coil drive circuit is as shown in Fig. 8. The analysis experiment results from the current characteristics are the magnetic flux for the current value of $3A$ at unaligned and aligned position is presented.It can be seen when the machine at unaligned position (a) the flux linkage around the machine is produces $0.6 - 0.8T$ and when the machine is at aligned position (b) the flux linkage around the stator is produces$1.2 - 1.6T$. It can be explain that when the machine is at aligned position the magnetic resistance is dominant; as the machine is at unaligned positions the current is gradually increases and the magnetic flux gradually decreases.

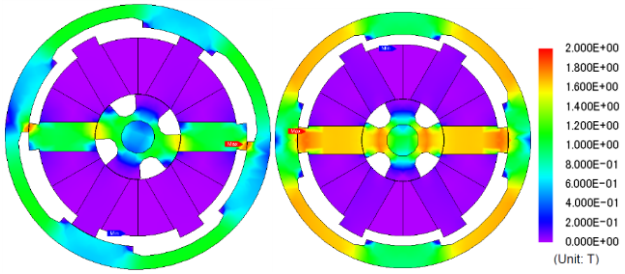

(a) unaligned (b) aligned

Fig. 8.Magnetic flux intensity.

4.3. Comparative evaluations

Figure 9 shows the machine static characteristics of the proposed machine with better torque from all the improved version of the SRM.

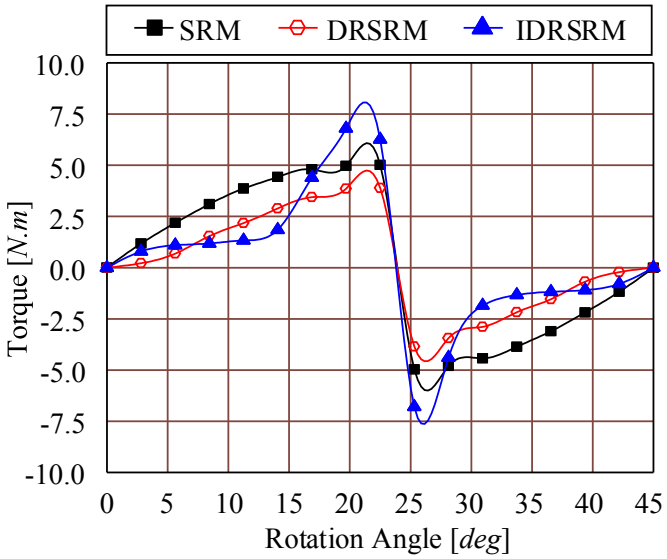

Fig. 9.Static torque characteristics.

Figure 10, the DRSRM shows that the machine design has the capabilities to reach steady state faster than the other two machines, moreover it has highest starting torque compare to the SRM and proposed machine.

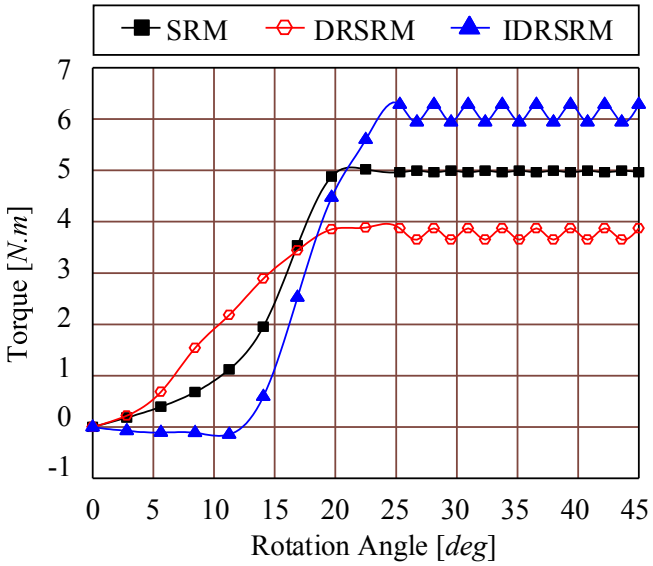

Fig. 10.Static comparison characteristics.

As seen from the Table 1 the comparative evaluation using motor torque constant square density as evaluations parameter. The average torque of the proposed machine structure is gradually increased over the conventional switched reluctance machine and double rotor switched reluctance machine. In addition, the motor torque constant square density value of the proposed machine showing an increase by twice of the conventional machine.

Table 1.Comparison on figures of merit.

Figure of Merit	*SRM*	*DRSRM*	*IDRSRM*
$I\ [A]$	5	5	5
$V\ [m^3]$	$2.13e^{-3}$	$2.20e^{-3}$	$1.99e^{-3}$
$T_{avg}[Nm]$	3.85	3.13	4.36
$K_t[Nm/A]$	0.77	0.63	0.87
$K_m\left[Nm/A/W^{-\left(\frac{1}{2}\right)}\right]$	0.077	0.063	0.087
$G\ [Nm^2/A^2/W/m^3]$	27.87	17.84	**38.20**

5. Conclusions

Dual magnetic circuit realization through double stator and double rotor are investigated these days. A double rotor system with dual magnetic circuit is realized of reluctance machines, a new double rotor switched reluctance machine.

The proposed design is structured, simulated, and evaluated using the standard finite element analysis through motor constant square density. The investigation shows that a percentage improvement in the motor constant square density by 37% in the comparison of SRM and 114% in the comparison of DRSRM and the improvement of the proposed IDRSRM. The average torque improved by 13% in comparison to the conventional SRM and 39% compared to that of the DRSRM.

References

1. C. Aravind Vaithilingam.; and C. Kamalakannan. (2003). *Design of Electrical Apparatus*. Chennai India: Charulatha Publications, India
2. Kumar, T.; Dinesh; and Nagarajan, A.(2013) Design of Switched Reluctance Motor for Elevator Application. *Journal of Asian Scientific Research,* 258-267.
3. Horst, G.; and French, A. (1997). Rotor position sensing in a dynamoelectric machine using coupling between machine coils.Patent US 5701064.
4. Cardenas, R.; Ray, W.F.; Asher, G.M. (1995). Switched reluctance generators for wind energy applications. *26th Annual IEEE Power Electronics Specialists Conference,* 1(1), 559-564.
5. Krishnan, R (2001). Switched Reluctance Motor Drives: Modelling Simulation, Analysis, Design, and Applications. BocaRaton, FL: CRC Press.

6. Aravind, C.V.; Norhisam, M.; Aris, I.; Marhaban, M.H. (2012). Computation of magnetic characteristics for the double rotor switched reluctance motor using flux tube analysis. Asia-Pacific Symposium on Applied Electromagnetics and Mechanics, Vietnam.
7. Mikail, R.; Husain, I; Sozer, Y.; Islam, M.; Sebastian, T. (2012). Four-quadrant torque ripple minimization of switched reluctance machine through current profiling with mitigation of rotor eccentricity problem and sensor errors. *IEEE Energy Conversion Congress and Exposition,* 838-842.
8. Mikail, R.; Sozer, Y.; Husain, I; Islam, M.; and Sebastian, T. (2011). Torque ripple minimization of switched reluctance machines through current profiling. *IEEEEnergy Conversion Congress and Exposition,* 3568-3574.
9. Blaabjerg, F.; Kjaer, P.C.; Rasmussen, P.O.; and Cossar, C. (1999). Improved digital current control methods in switched reluctance motor drives.*IEEE Transactions on Power Electronics,* 14(3), 563,572.
10. Aravind, C.V.; Norhisam, M,Marhaban, M.H.; and Aris, I. (2012). Analytical Design of Double Rotor Switched Reluctance Motor using Optimal Pole Arc Values.*International Review in Electrical and Electronics*, 7(1),3314-3324.
11. Grace, I; Teymourzadeh, R.; Bright, S.; and Aravind, C.V. (2011).Optimised toolbox for the design of rotary reluctance motors. *IEEE International Conference on Sustainable Utilization and Development in Engineering and Technology,* 1-6.
12. Aravind, C.V.; Grace, I; Rozita, T.; Rajparthiban, R.; Rajprasad, R.; Wong, Y.V. (2012). Universal computer aided design for electrical machines. *, 8th International IEEE Colloquium on Signal Processing and its Applications*, 99-104.
13. Aravind, C.V.; Norhisam, M.; Aris, I.; Ahmad, D.; and Nirei, M. (2011). Double Rotor Switched Reluctance Motors: Fundamentals and magnetic circuit analysis. *IEEE Student Conference on Research and Development,* 294-299.
14. Chockalingam, Aravind Vaithilingam.;Norhisam,Misron.; Mohammad, Reza Zare.;Ishak,Aris.; and Mohammad,HamiruceMarhaban. (2012). Computation of Electromagnetic Torque in a Double Rotor Switched Reluctance Motor Using Flux Tube Methods. *Energies.* 5(10), 4008-4026.
15. Chockalingam, Aravind Vaithilingam.; Norhisam ,Misron.; Ishak, Aris.; Mohammad, HamiruceMarhaban.; and Masami, Nirei. (2013). Electromagnetic Design and FEM Analysis of a Novel Dual air-gap Reluctance Machine. *Progress in Electromagnetics Research.* 140(1), 523-544.